

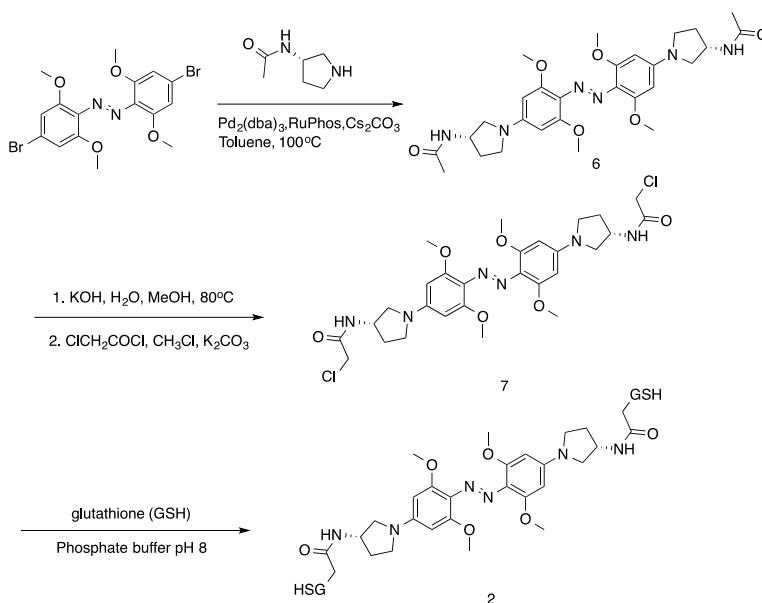
Supplementary information for:

Red, far-red, and near infrared photoswitches based on azonium ions

M. Dong, A. Babalhavaeji, M. Hansen, L. Kálmán^b and G. A. Woolley^a

Synthetic methods

General aspects: All commercial materials (solvents, reagents and substrates) were used as received. The NMR spectra were recorded either on Varian Vnmr-S 400 MHz or Varian Mercury 400 MHz or Varian UnityPlus 500 MHz or Agilent 600 or 700 MHz spectrometers. Silica gel of particle size 40-63 μm from Silicycle Chemical Division was used for all column chromatography.



Scheme S1. The synthesis of compound 2

Synthesis of N,N'-((3S, 3'S)-((-diazene-1,2-diyl)bis(3,5-dimethoxy-4,1-phenylene))bis(pyrrolidine-1,3-diyl))diacetamide (6):

To an oven-dried pressure tube, cooled under nitrogen gas, was added 1,2-bis(4-bromo-2,6-dimethoxyphenyl)diazene (46 mg, 0.1 mmol), 1-[(3s)-3-pyrrolidinyl]acetamide (39 mg, 0.3 mmol), Pd₂(dba)₃ (9 mg, 0.01 mmol), followed by Cs₂CO₃ (98 mg, 0.3 mmol), RuPhos (9.3 mg, 0.02 mmol), and toluene (5 mL). After flushing with nitrogen gas, the tube was capped with a Teflon stopper and heated at 100°C for 18h. The reaction was cooled to room temperature and extracted with ethyl acetate. The combined organic layers were washed with brine, dried over anhydrous Na₂SO₄ and concentrated under vacuum. The crude product was subjected to silica gel column chromatography (eluent: chloroform: methanol= 3: 1) to isolate **6** (52 mg, 94% yield) as a blue solid. ¹H NMR (400 MHz, methanol-*d*₄) δ ppm 1.98 (s, 6H), 2.20 (m, 4H), 3.62 (m, 4H), 3.75 (m, 2H), 4.01 (s, 12H), 4.38 (m, 4H), 5.81 (s, 4H); ¹³C NMR (500 MHz, DMSO-*d*₆) δ ppm 22.9, 31.0, 49.0, 55.2, 56.9, 67.5, 90.9, 119.2, 149.7, 161.6, 170.3; MALDI-MS: m/z calc'd for C₂₈H₃₉N₆O₆: 555.3 [M+H]⁺; found: 555.6.

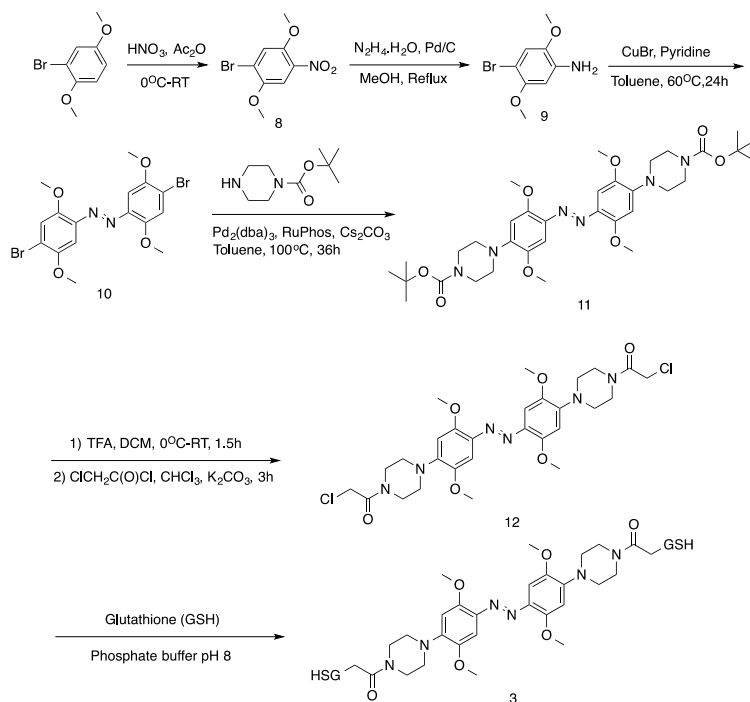
Synthesis of N,N'-((3S, 3'S)-((-diazene-1,2-diyl)bis(3,5-dimethoxy-4,1-phenylene))bis(pyrrolidine-1,3-diyl))bis(2-chloroacetamide) (7):

To a solution of potassium hydroxide (1.12 g, 20 mmol) in water (5 mL) and methanol (5 mL) was added compound **6** (52 mg, 0.093 mmol), the resulting solution was stirred at 80°C for 48 hour. Then, it was cooled to 0°C and α-chloroacetyl chloride (56 mg, 0.5 mmol) was added dropwise, the reaction was stirred at room temperature for 3h. The reaction solution was extracted with ethyl acetate, and the combined organic layers were washed with brine, dried over anhydrous Na₂SO₄ and concentrated under vacuum. The crude product was subjected to silica

gel column chromatography (eluent: chloroform: methanol= 3: 1) to isolate **7** (27 mg, 47% yield) as a blue solid. ^1H NMR (400 MHz, DMSO- d_4) δ ppm 1.92 (m, 2H), 2.20 (m, 2H), 3.15 (m, 2H), 3.40 (m, 6H), 3.57 (m, 2H), 3.66 (s, 12H), 4.04 (s, 4H), 4.40 (m, 2H), 5.80 (s, 4H); ^{13}C NMR (125 MHz, DMSO- d_4) δ ppm 21.0, 30.9, 43.0, 46.3, 48.9, 49.5, 53.5, 56.5, 62.5, 90.0, 126.1, 148.5, 154.3, 170.4; DART-HRMS: m/z calc'd for $\text{C}_{28}\text{H}_{37}\text{Cl}_2\text{N}_6\text{O}_6$: 623.2152 $[\text{M}+\text{H}]^+$; found: 623.2140.

Synthesis of the glutathione adduct compound (2):

To a solution of glutathione (9.3 mg in 2.4 mL 100 mM sodium phosphate buffer at pH 8) was added a solution of compound **7** (6.2mg in 1.6 mL DMSO). The resulting reaction was stirred at 45°C under a nitrogen atmosphere for 18h. The completion of the reaction was judged by MALDI-MS. The reaction was dried under high vacuum, and the cross-linked peptide was purified by reverse-phase HPLC (Zorbax SB-C18 column with a linear gradient from 5% to 70% acetonitrile/ water containing 0.1% formic acid over 25 min). The cross-linked peptide composition was confirmed by MALDI-MS: m/z calc'd for $\text{C}_{48}\text{H}_{69}\text{N}_{12}\text{O}_{18}\text{S}_2$: 1165.4 $[\text{M}+\text{H}]^+$; found: 1165.5.



Scheme S2. The synthesis of compound **3**

Synthesis of 1-bromo-2,5-dimethoxy-4-nitrobenzene (**8**):

To an ice-cold solution of 1-bromo-2,5-dimethoxybenzene (Sigma-Aldrich) (5.03 g, 23.18 mmol) in acetic anhydride (50.0 mL) was added dropwise conc. HNO_3 (3.46 mL, 50.0 mmol) over a period of 30 min. The resulting solution was stirred at 0°C for 1 hour and at room temperature overnight. It was then poured into ice-water with vigorous stirring; the solution was filtered, washed with water and dried under high vacuum. The yellow solid **8** (5.03 g, 83% yield) was obtained, which was pure enough for the next reaction. ^1H NMR (400 MHz, chloroform-*d*) δ ppm 3.92 (s, 3H), 3.94 (s, 3H), 7.34 (s, 1H), 7.47 (s, 1H); ^{13}C NMR (100 MHz, chloroform-*d*) δ ppm 57.0, 57.4, 108.7, 118.6, 119.3, 138.2, 147.6, 149.6; DART-HRMS: m/z calc'd for $\text{C}_8\text{H}_9\text{BrNO}_4$: 261.97150 $[\text{M}+\text{H}]^+$; found: 261.97139.

Synthesis of 4-bromo-2,5-dimethoxyaniline (9):

To a solution of 1-bromo-2,5-dimethoxy-4-nitrobenzene (5 g, 19.08 mmol) in methanol (100 mL) was added hydrazine hydrate (50-60wt%, 7.6 mL, about 76.34 mmol) and Pd/C(10wt%, 0.25 g). The resulting heterogeneous reaction mixture was heated to reflux overnight. After cooling, the reaction was filtered, washed with methanol and concentrated to about 20mL. The solution was filtered again, washed with water and dried under high vacuum. The pale green solid **9** (2.07 g, 47% yield) was obtained, which was pure enough for the next reaction. ¹H NMR (400 MHz, chloroform-*d*) δ ppm 3.80 (s, 6H), 6.37 (s, 1H), 6.93 (s, 1H); ¹³C NMR (100 MHz, chloroform-*d*) δ ppm 56.3, 56.9, 97.9, 100.5, 115.7, 136.4, 141.8, 150.5; DART-HRMS: m/z calc'd for C₈H₁₁BrNO₂: 231.99732 [M+H]⁺; found: 231.99728.

Synthesis of 1,2-bis(4-bromo-2,5-dimethoxyphenyl)diazene (10):

Copper bromide (CuBr) (0.68 g, 4.74 mmol), pyridine (0.75 g, 9.48 mmol), and 4-bromo-2,5-dimethoxyaniline (1.1 g, 4.74 mmol) were mixed in toluene (60 mL) under air (1 atm). The reaction mixture was vigorously stirred at 60 °C for 24 h. After cooling to room temperature and concentrating under vacuum, the residue was purified by flash chromatography on a short silica gel (eluent: chloroform: ethyl acetate: hexanes= 1: 1: 1) to afford 406 mg (37%) of the red solid **10**. ¹H NMR (400 MHz, chloroform-*d*) δ ppm 3.92 (s, 6H), 3.99 (s, 6H), 7.29 (s, 2H), 7.32 (s, 2H); ¹³C NMR (100 MHz, chloroform-*d*) δ ppm 56.8, 57.2, 100.2, 116.3, 118.3, 141.8, 150.6, 151.7; DART-HRMS: m/z calc'd for C₁₆H₁₇Br₂N₂O₄: 460.95346 [M+H]⁺; found: 460.95346.

Synthesis of di-tert-butyl-4,4'-(diazene-1,2-diylbis(2,5-dimethoxy-4,1-phenylene))bis-piperazine-1-carboxylate (11):

To an oven-dried pressure tube, cooled under nitrogen gas, was added **10** (46 mg, 0.1 mmol), *tert*-butyl piperazine-1-carboxylate (56 mg, 0.3 mmol), Pd₂(dba)₃ (9 mg, 0.01 mmol), followed by Cs₂CO₃ (98 mg, 0.3 mmol), RuPhos (9.3 mg, 0.02 mmol), and toluene (5 mL). After flushing with nitrogen gas, the tube was capped with a Teflon stopper and heated at 100°C for 36h. The reaction was cooled to room temperature and extracted with ethyl acetate. The combined organic layers were washed with brine, dried over anhydrous Na₂SO₄ and concentrated under vacuum. The crude product was subjected to silica gel column chromatography (eluent: chloroform: methanol= 100: 1) to isolate **11** (55 mg, 82% yield) as a dark red solid. ¹H NMR (400 MHz, chloroform-*d*) δ ppm 1.49 (s, 18H), 3.13 (t, 8H, *J* = 5.0 Hz), 3.63 (t, 8H, *J* = 5.0 Hz), 3.90 (s, 6H), 4.00 (s, 6H), 6.58 (s, 2H), 7.35 (s, 2H); ¹³C NMR (100 MHz, chloroform-*d*) δ ppm 28.5, 50.4, 55.9, 57.6, 77.2, 79.9, 100.1, 104.1, 137.7, 144.9, 146.9, 152.5, 154.7; DART-HRMS: *m/z* calc'd for C₃₄H₅₁N₆O₈: 671.37684 [M+H]⁺; found: 671.38658.

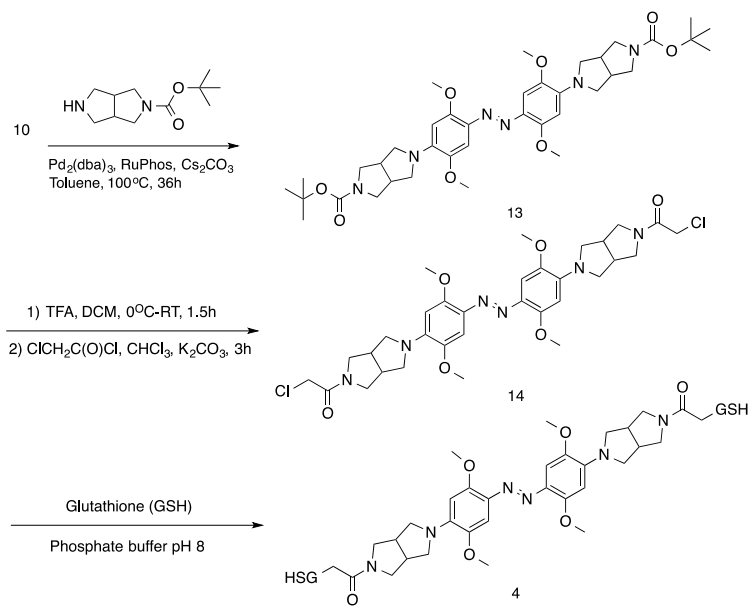
Synthesis of 4,4'-(diazene-1,2-diylbis(2,5-dimethoxy-4,1-phenylene))bis(piperazine-4,1-diyl))bis-2-chloroethanone (12):

To a solution of **11** (55 mg, 0.08 mmol) in dichloromethane (5 mL) was added trifluoroacetic acid (1 mL) at 0°C. The resulting reaction was stirred at room temperature for 0.5h and concentrated under high vacuum to afford the deprotected amine as a blue solid, which was pure enough for the next reaction. The solid was redissolved in chloroform (10 mL) and treated with NEt₃ (50 mg, 0.5 mmol). After stirring for 15 minutes at room temperature, it was cooled to 0°C and a solution of α-chloroacetyl chloride (28 mg, 0.25 mmol) in chloroform (1 mL) was added

dropwise. The reaction was stirred at room temperature for 3h and concentrated under high vacuum. The crude product was purified using silica gel column chromatography (eluent: chloroform: methanol= 50: 1) to afford **12** as a dark red solid (35 mg, 69% yield over two steps). ¹H NMR (400 MHz, chloroform-*d*) δ ppm 3.19 (t, 4H, *J* = 5.0 Hz), 3.25 (t, 4H, *J* = 5.0 Hz), 3.73 (t, 4H, *J* = 5.0 Hz), 3.84 (t, 4H, *J* = 5.0 Hz), 3.91 (s, 6H), 4.01 (s, 6H), 4.10 (brs, NH⁺), 4.13 (s, 4H), 6.58 (s, 2H), 7.36 (s, 2H); ¹³C NMR (100 MHz, chloroform-*d*) δ ppm 40.8, 42.2, 46.5, 49.9, 50.5, 55.9, 57.7, 100.2, 104.3, 137.9, 144.3, 146.8, 152.5, 165.2; DART-HRMS: *m/z* calc'd for C₂₈H₃₇N₆O₆Cl₂: 623.2151 [M+H]⁺; found: 623.2130.

Synthesis of the glutathione adduct compound (3):

To a solution of glutathione (8.9 mg in 1.2 mL 100 mM sodium phosphate buffer at pH 8) was added the solution of compound **12** (3 mg in 0.8 mL DMSO), the resulting reaction was stirred at 45°C under a nitrogen atmosphere for 18 hour. The completion of the reaction was judged by MALDI-MS. The reaction was dried under high vacuum, and the cross-linked peptide was purified by reverse-phase HPLC (Zorbax SB-C18 column with a linear gradient from 5% to 70% acetonitrile/ water containing 0.1% trifluoroacetic acid over 25-min). The cross-linked peptide composition was confirmed by MALDI-MS: *m/z* calc'd for C₄₈H₆₉N₁₂O₁₈S₂: 1165.5 [M+H]⁺; found: 1165.6.



Scheme S3. The synthesis of compound **4**

**Synthesis of tert-butyl 5,5'-(4,4'-(diazene-1,2-diyl)bis(2,5-dimethoxy-4,1-phenylene))Bis
(hexahydropyrrolo[3,4-c]pyrrole-2(1H)-carboxylate)(13)**

To an oven-dried pressure tube, cooled under nitrogen gas, was added **10** (23 mg, 0.05 mmol), 2-Boc-hexahydro-pyrrolo[3, 4-C]pyrrole (32 mg, 0.15 mmol), Pd₂(dba)₃ (9 mg, 0.01 mmol), followed by Cs₂CO₃ (49 mg, 0.15 mmol), RuPhos (9.3 mg, 0.02 mmol), and toluene (5 mL). After flushing with nitrogen gas, the tube was capped with a Teflon stopper and heated at 100°C for 12h. The reaction was cooled to room temperature and extracted with ethyl acetate. The combined organic layers were washed with brine, dried over anhydrous Na₂SO₄ and concentrated under vacuum. The crude product was subjected to silica gel column chromatography (eluent: chloroform: acetone= 1: 1) to isolate **13** (30 mg, 83% yield) as a dark red solid. ¹H NMR (400 MHz, chloroform-*d*) δ ppm 1.47 (s, 18H), 2.95 (m, 4H), 3.35 (m, 8H), 3.63 (m, 4H), 3.73 (m, 4H), 3.84 (s, 6H), 4.00 (s, 6H), 6.27 (s, 2H), 7.41 (s, 2H); ¹³C NMR (100

MHz, chloroform-*d*) δ ppm 28.5, 41.0, 42.0, 50.5, 55.0, 56.2, 57.5, 100.4, 142.1, 144.6, 152.8, 154.6; DART-HRMS: m/z calc'd for $C_{38}H_{55}N_6O_8$: 723.40031 $[M+H]^+$; found: 722.40937.

Synthesis of 1, 1'-(5,5'-(4,4'-(diazene-1,2-diyl)bis(2,5-dimethoxy-4,1-phenylene))Bis(hexahydropyrrolo[3,4-c]pyrrole-5,2(1H)-diyl))bis(2-chloroethanone) (14)

To a solution of **13** (30 mg, 0.04 mmol) in chloroform (5 mL) was added trifluoroacetic acid (1 mL) at 0°C. The resulting reaction was stirred at room temperature for 0.5h and concentrated under high vacuum to afford the deprotected amine as a blue solid, which was pure enough for the next reaction. The solid was redissolved in chloroform (10 mL) and treated with NEt_3 (70 μ L, 0.5 mmol). After stirring for 15 minutes at room temperature, it was cooled to 0°C and a solution of α -chloroacetyl chloride (45 mg, 0.4 mmol) in chloroform (1 mL) was added dropwise. The reaction was stirred at room temperature for 3h and concentrated under high vacuum. The crude product was purified using silica gel column chromatography (eluent: chloroform: acetone= 1: 1) to afford **14** as a dark red solid (18 mg, 66% yield over two steps). 1H NMR (400 MHz, DMSO-*d*₆) δ ppm 3.00 (m, 4H), 3.36 (m, 8H), 3.66 (m, 8H), 3.72 (s, 6H), 3.92 (s, 6H), 4.34 (s, 4H), 6.34 (s, 2H), 7.21 (s, 2H); ^{13}C NMR (100 MHz, DMSO-*d*₆) δ ppm 41.9, 42.3, 50.9, 56.2, 57.4, 100.4, 141.8, 144.6, 152.6, 164.9; DART-HRMS: m/z calc'd for $C_{32}H_{41}N_6O_6Cl_2$: 675.2459 $[M+H]^+$; found: 675.2453.

Synthesis of the glutathione adduct, compound (4):

To a solution of glutathione (5.5 mg in 1.5 mL 100 mM sodium phosphate buffer at pH 8) was added a solution of compound **14** (2 mg in 1.0 mL DMSO), the resulting reaction was stirred at 45°C under a nitrogen atmosphere for 18 hour. The completion of the reaction was judged by MALDI-MS. The reaction was dried under high vacuum, and the cross-linked peptide was

purified by reverse-phase HPLC (Zorbax SB-C18 column with a linear gradient from 5% to 70% acetonitrile/ water containing 0.1% trifluoroacetic acid over 25-min elution). The cross-linked peptide composition was confirmed by MALDI-MS: m/z calc'd for $C_{52}H_{73}N_{12}O_{18}S_2$: 1217.5 $[M+H]^+$; found: 1217.5.

Sample preparation for UV-Visible spectroscopy

Solutions were prepared in a mixture of four buffers (CAPSO, TRIS, MES, sodium acetate, 25 mM each) to ensure the pH could be easily adjusted between 2 and 11 by addition of small quantities of concentrated hydrochloric acid and sodium hydroxide. The pH was measured by a glass combination micro-electrode (MI-710, Microelectrodes Inc.)

Calculation of molar extinction coefficients

Absorbance spectra of the GSH adduct of each compound (**1-4**) in a 1 cm quartz cell were obtained in the universal buffer solution described above using a Perkin Elmer Lambda-35 instrument coupled to a Peltier temperature controller (Quantum Northwest). The concentration of the samples was then determined by quantitative amino acid analysis using a Water Pico-tag system as follows (performed at the SPARC BioCentre at the Hospital for Sick Children, Toronto): Samples were dried in pyrolyzed borosilicate tubes in a vacuum centrifugal concentrator and subjected to vapour phase hydrolysis by 6N HCl with 1% phenol at 110°C for 24 hours under a pre-purified nitrogen atmosphere. After hydrolysis, excess HCl was removed by vacuum, hydrolyzates were washed with redrying solution (Waters, Inc) and derivatized with phenylisothiocyanate (PITC) to produce phenylthiocarbamyl (PTC) amino acids. Derivatized amino acids are redissolved in phosphate buffer and transferred to injection vials which are loaded into an autosampler for automatic injection. PTC derivatives were separated by reverse phase HPLC. PTC derivatives of Gly and Glu (derived from hydrolysis of GSH) were quantified by comparison with standards. Molar extinction coefficients at a given wavelength were calculated by dividing absorbance values determined by UV-Vis measurements by concentrations determined by quantitative amino acid analysis. Note that estimation of azonium ion extinction coefficients is complicated by the possible coexistence of doubly protonated species (see text).

pH-dependence of absorption spectra

UV-Visible spectra were acquired using a Perkin Elmer Lambda-1050 instrument coupled to a Peltier temperature controller (PTP-6, Perkin Elmer). The temperature was maintained at 20 degrees. All spectra were baseline-corrected, assuming zero absorption at 800 nm. To estimate the apparent pK_a 's for the trans form of each compound, the absorbance values at the maximum absorption wavelengths corresponding to the azonium ions (Table I) were plotted against the pH. For compounds **1**, **2**, and **3** these data were fitted to Eq. 1, which describes a single protonation event.

$$Abs_{\lambda} = [A]_{tot} \left(\epsilon_A \left(1 - \left(1 / (1 + 10^{(pH-pK_a)}) \right) \right) + \epsilon_{HA} \left(1 / (1 + 10^{(pH-pK_a)}) \right) \right) \quad \text{Eq. 1}$$

Where $[A]_{tot}$ is the total concentration of the compound (in any ionization state), ϵ_A is the molar extinction coefficient of the neutral species, ϵ_{HA} is the molar extinction coefficient of the singly protonated azonium ion. For compound **4**, data were fitted to Eq. 2, which describes two protonation events:

$$Abs_{\lambda} = [A]_{tot}(\epsilon_A(f_N) + \epsilon_{HA}(f_{P1}) + \epsilon_{HHA}(f_{P2})) \quad \text{Eq. 2}$$

Where ϵ_{HHA} is the molar extinction coefficient of the doubly protonated azonium/ammonium ion and f_N, f_{P1}, f_{P2} are the fractions of neutral, singly protonated and doubly protonated species respectively:

$$f_N = 10^{(pH-pK2)} \cdot 10^{(pH-pK1)} / (10^{(pH-pK2)} + 1 + (10^{(pH-pK2)} \cdot 10^{(pH-pK1)}))$$

$$f_{P1} = 10^{(pH-pK2)} / (10^{(pH-pK2)} + 1 + (10^{(pH-pK2)} \cdot 10^{(pH-pK1)}))$$

$$f_{P2} = 1 / (10^{(pH-pK2)} + 1 + (10^{(pH-pK2)} \cdot 10^{(pH-pK1)}))$$

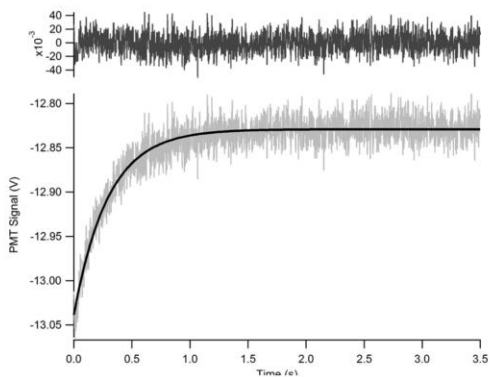
The constants pK_1 and pK_2 refer to the dissociation of the single protonated and doubly protonated species respectively.

Thermal relaxation kinetics for **2**

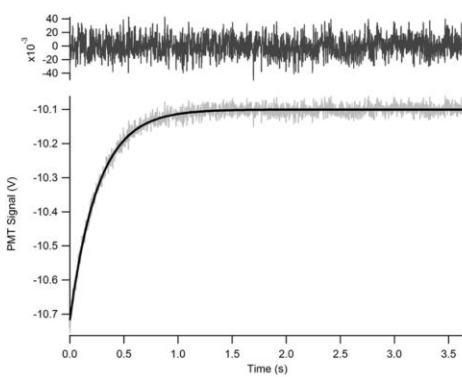
A solution of **2** was prepared in the buffer mixture described above. For each measurement, fresh samples with a known pH were injected into a Z-shaped flow cell (FIALab) with a light path length of 2.5 mm. A 530 nm LED, 700 mA, 5.6 mW/cm² was used as a source for the measuring beam while isomerization was achieved by irradiation with 455 nm (Thorlabs) or 660 nm (Mightex Systems Inc.) high power LEDs.

Thermal relaxation rates were measured by monitoring absorbance after removal of the blue light source. Relative absorbance values were recorded using a photomultiplier tube (Oriel, Newport Corporation) connected to a digital oscilloscope (Handyscope HS3, TiePie Engineering). Two linear variable band-pass filters (LVF-HL, Ocean Optics) transmitting at 540 nm \pm 20nm were placed before and in front of the sample to eliminate other wavelengths, including scattered light coming from the isomerization light source. A third band-pass filter transmitting at 530nm \pm 20nm (QuantaMax) was placed in front of the detector to further block the scattered blue light. The output of the detector was recorded immediately after triggering the blue light off. Fitting the photomultiplier tube signal vs. elapsed time to a monoexponential decay process gave the observed kinetic constants for thermal relaxation at various pHs. These data are shown in Figure S2. Kinetic constants used were the average of at least three decay curves. The temperature of the sample was maintained near 22 °C during all measurements. To confirm that the rate of cis to trans conversion was dominated by thermal relaxation, relaxation rates were measured at two

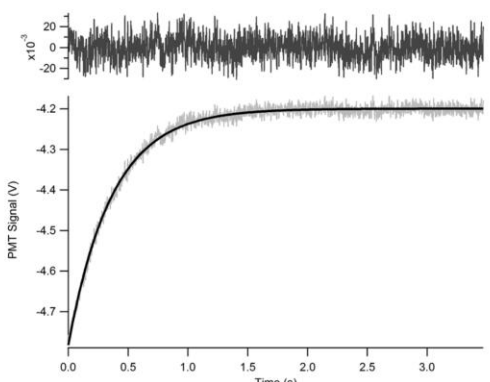
different intensities of the incident beam. Also, other wavelengths of the measuring beam were examined. Data obtained in these tests confirmed that the measuring beam used in this case does not significantly affect the observed rates.



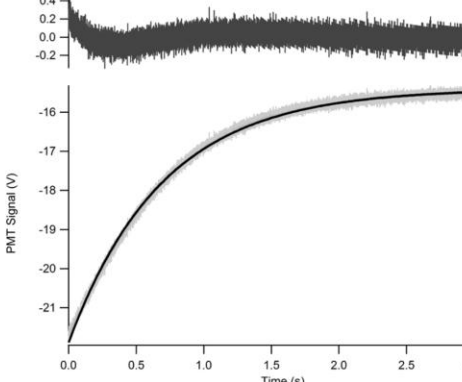
a. pH=6.9; $k=3.61 \text{ s}^{-1}$



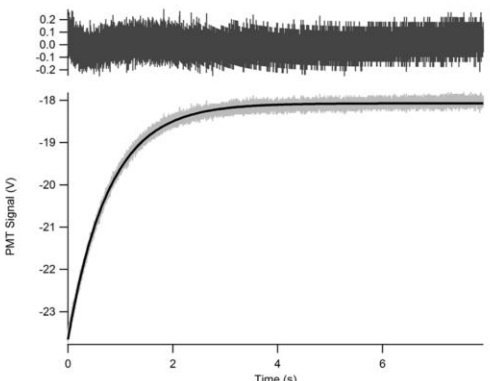
b. pH=7.5; $k=3.70 \text{ s}^{-1}$



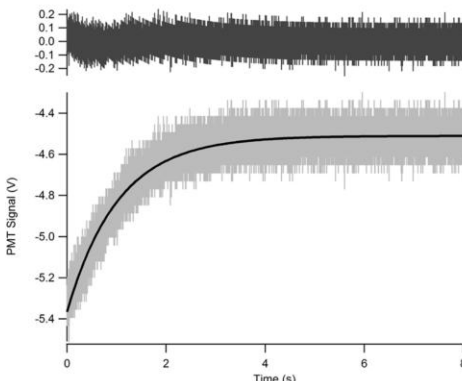
c. pH=8.2; $k=2.79 \text{ s}^{-1}$



d. pH=8.7; $k=1.40 \text{ s}^{-1}$



e. pH=8.9; $k=1.30 \text{ s}^{-1}$



f. pH=9.2; $k=1.02 \text{ s}^{-1}$

Laser flash photolysis experiments

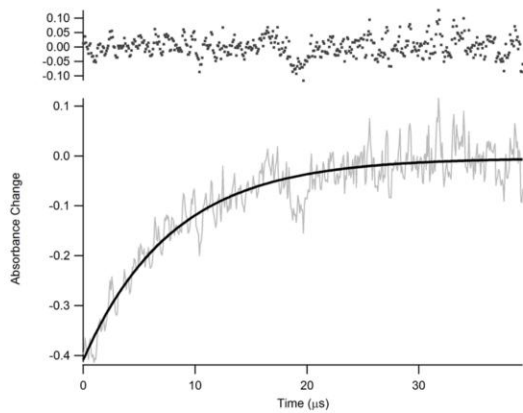
Solutions of **3** and **4** were prepared as described above and placed in a 1 cm quartz cuvette at room temperature (~22°C).

The isomerization rates of these two compounds were measured with a miniaturized laser-flash photolysis system (LFP-112; Luzchem Research Inc. Ottawa, ON, Canada) as described earlier⁴. Samples were excited with pulses of 25 mJ/pulse output energy and 3-5 ns pulse width at 532 nm from a frequency doubled Nd:YAG laser (Minilite II; Continuum, Santa Clara, CA, U.S.A.) The laser was operated with a 1 Hz repetition rate to allow plenty of time to the transitional signals to recover.

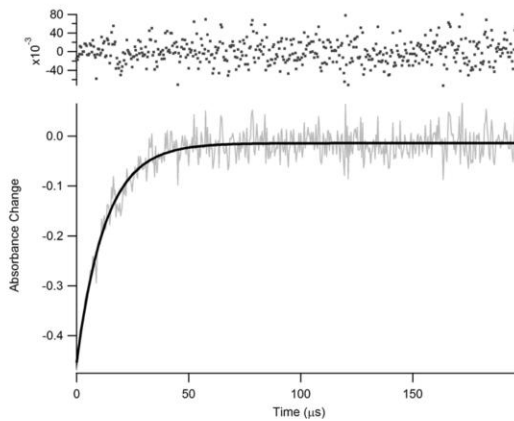
Various measuring beam wavelengths were tried between 380 nm to 700 nm to obtain an acceptable signal to noise ratio as the differential absorption spectra of trans and cis species were unknown. Eventually, transient measurements were carried out at 550nm for **3** and 480nm for **4**. 25 measurements were averaged for **3** at each pH point. The number of measurements that were averaged for **4** varied between 10 to 50 depending on the relaxation rate and the signal-to-noise at a given pH. The reproducibility of the kinetic traces indicated that numerous cycles of photoisomerization could be repeated without significant photobleaching.

Relaxation data were fit to single exponential functions to obtain decay rate constants at each pH.

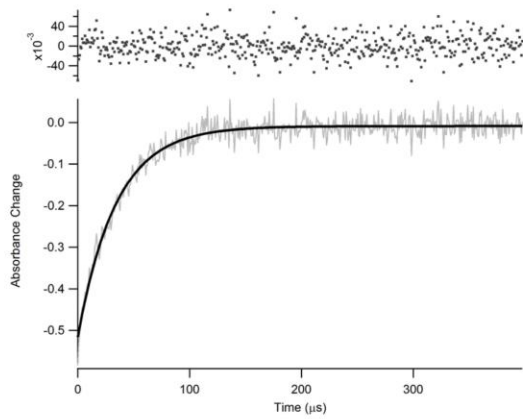
These data are shown in Figures S3 and S4. As with compound **2** (Fig. S2 above), it can be seen that relaxation data at most pHs is dominated by a single exponential decay process. We assume the time constant derived from these fits corresponds to the cis-to-trans thermal isomerization rate constant because this is expected to be much larger than the trans-to-cis rate constant. This is because calculations indicate the trans azonium ions (and neutral species) are ~10-15 kcal/mol more stable than the cis species.



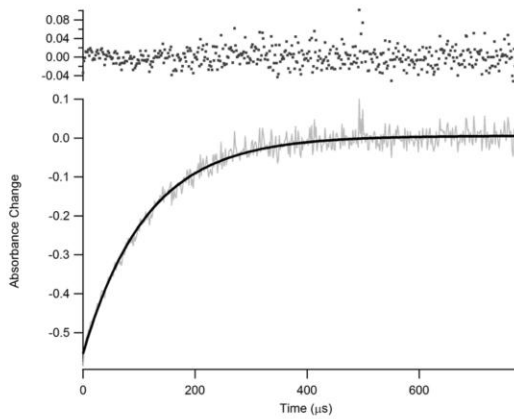
a. pH=3.9; 25 shots; $k=1.26 \times 10^5 \text{ s}^{-1}$



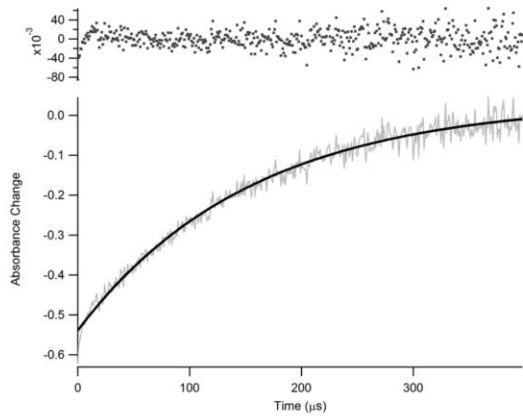
b. pH=4.3; 25 shots; $k=7.79 \times 10^4 \text{ s}^{-1}$



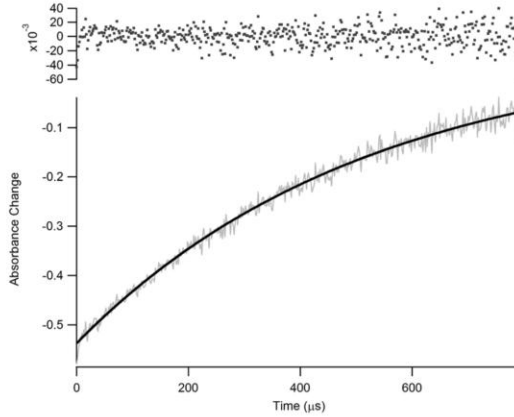
c. pH=4.8; 25 shots; $k=2.92 \times 10^4 \text{ s}^{-1}$



d. pH=5.3; 25 shots; $k=8.80 \times 10^3 \text{ s}^{-1}$



e. pH=5.7; 25 shots; $k=6.47 \times 10^3 \text{ s}^{-1}$



f. pH=6.1; 25 shots; $k=1.93 \times 10^3 \text{ s}^{-1}$

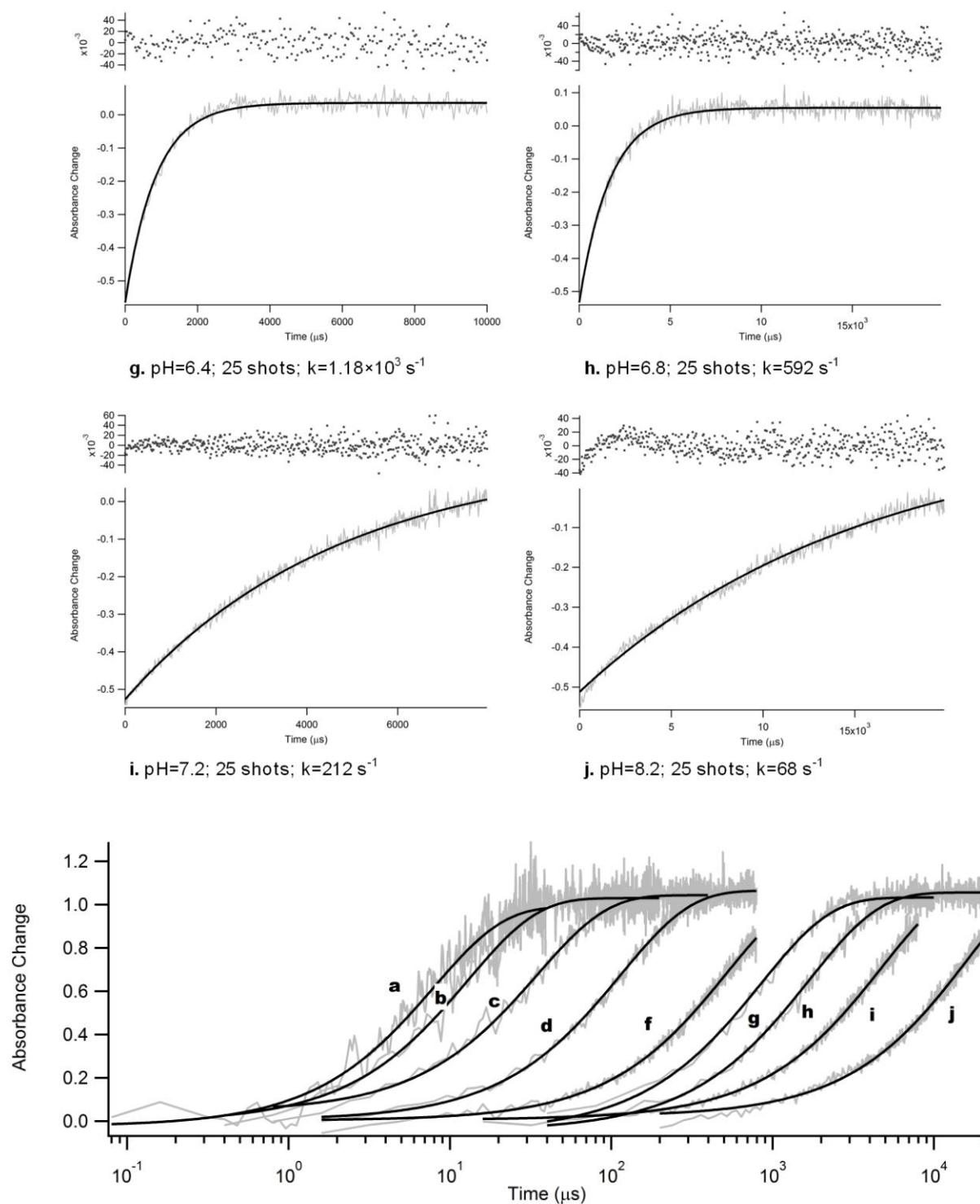
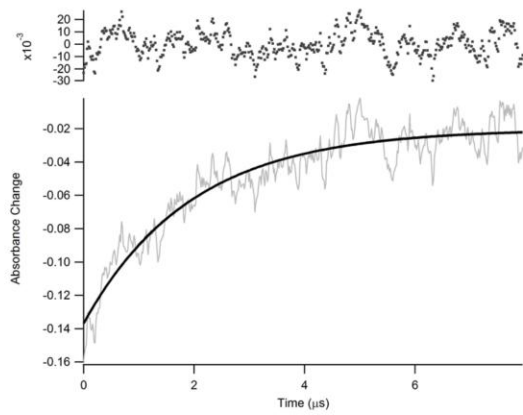
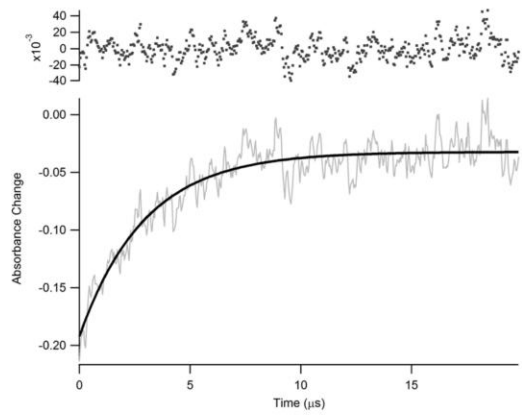


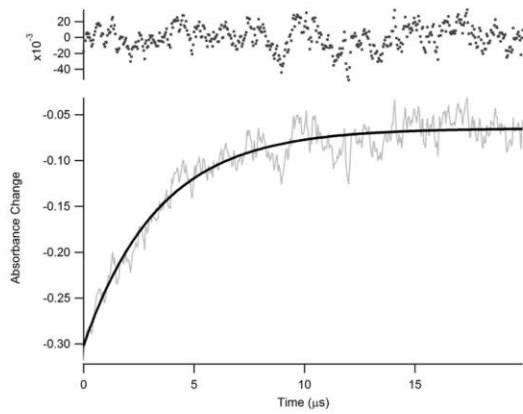
Figure S3. Thermal relaxation data for compound **3**. Each panel shows data obtained at the pH indicated below the panel. Monoexponential fits are shown together with calculated residuals. The time constant obtained (k) is listed below each panel. Selected traces are shown plotted together in the final panel with a logarithmic time axis.



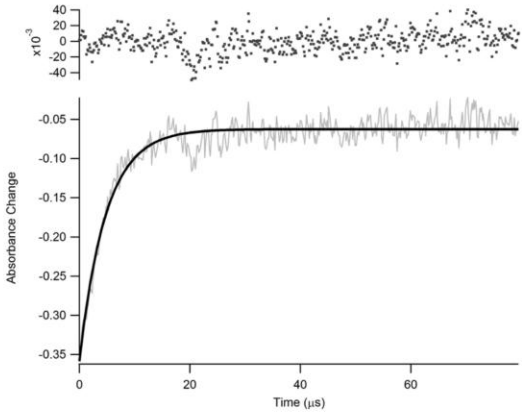
a. pH=4.8; 30 shots; $k=5.16 \times 10^5 \text{ s}^{-1}$



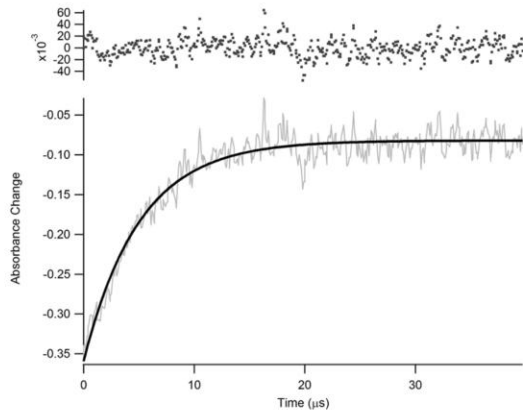
b. pH=5.1; 30 shots; $k=3.40 \times 10^5 \text{ s}^{-1}$



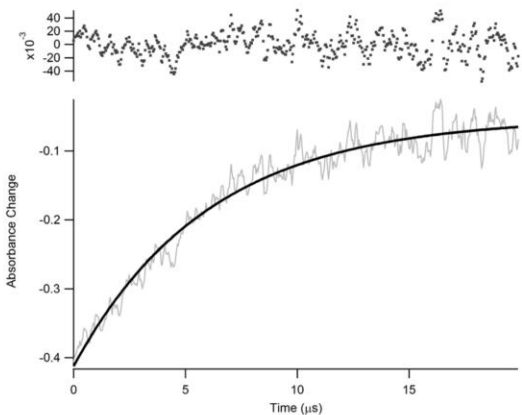
c. pH=5.6; 30 shots; $k=2.94 \times 10^5 \text{ s}^{-1}$



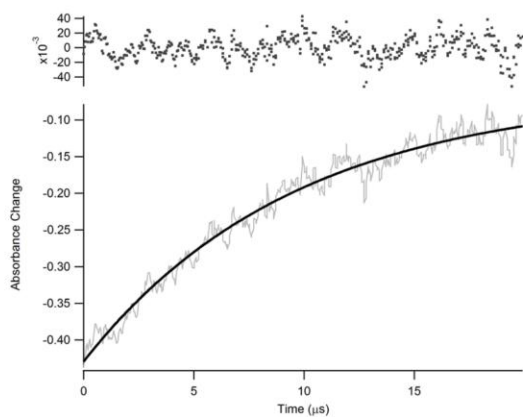
d. pH=6.1; 50 shots; $k=2.09 \times 10^5 \text{ s}^{-1}$



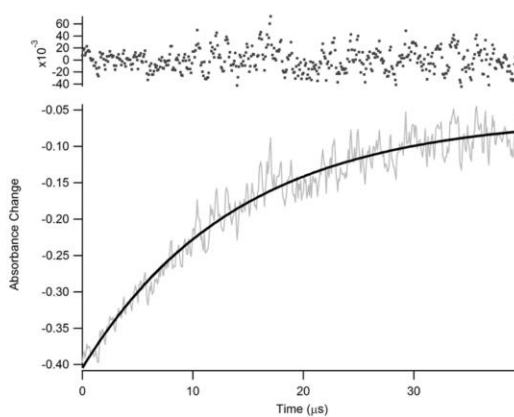
e. pH=6.3; 30 shots; $k=1.98 \times 10^5 \text{ s}^{-1}$



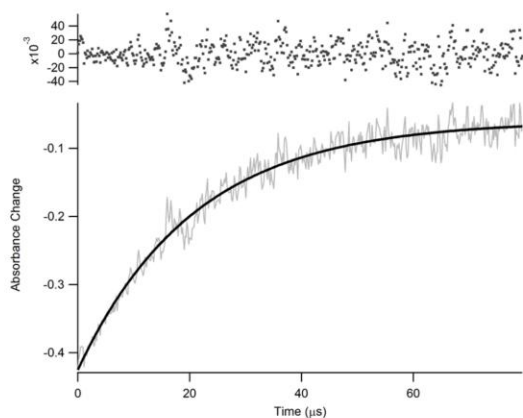
f. pH=6.5; 30 shots; $k=1.66 \times 10^5 \text{ s}^{-1}$



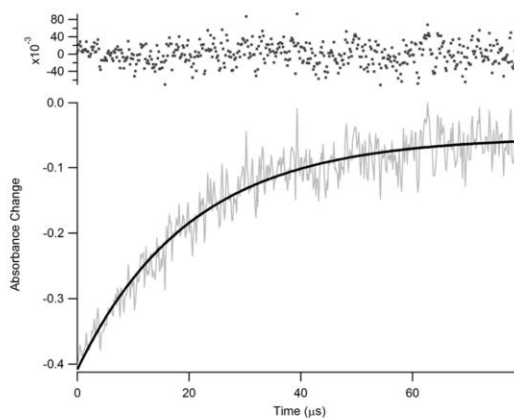
g. pH=7.1; 30 shots; $k=1.05 \times 10^5 \text{ s}^{-1}$



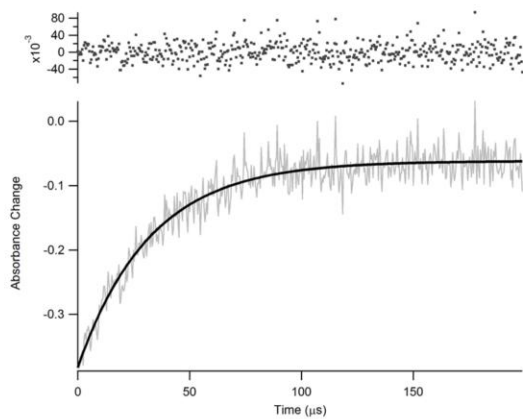
h. pH=7.6; 20 shots; $k=7.17 \times 10^4 \text{ s}^{-1}$



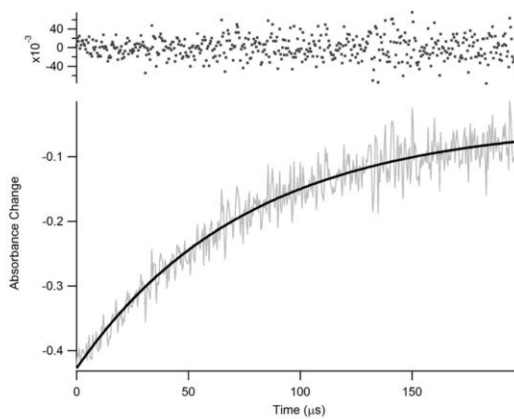
i. pH=8.0; 50 shots; $k=4.79 \times 10^4 \text{ s}^{-1}$



j. pH=8.1; 10 shots; $k=4.97 \times 10^4 \text{ s}^{-1}$



k. pH=8.4; 10 shots; $k=3.11 \times 10^4 \text{ s}^{-1}$



l. pH=8.9; 10 shots; $k=1.32 \times 10^4 \text{ s}^{-1}$

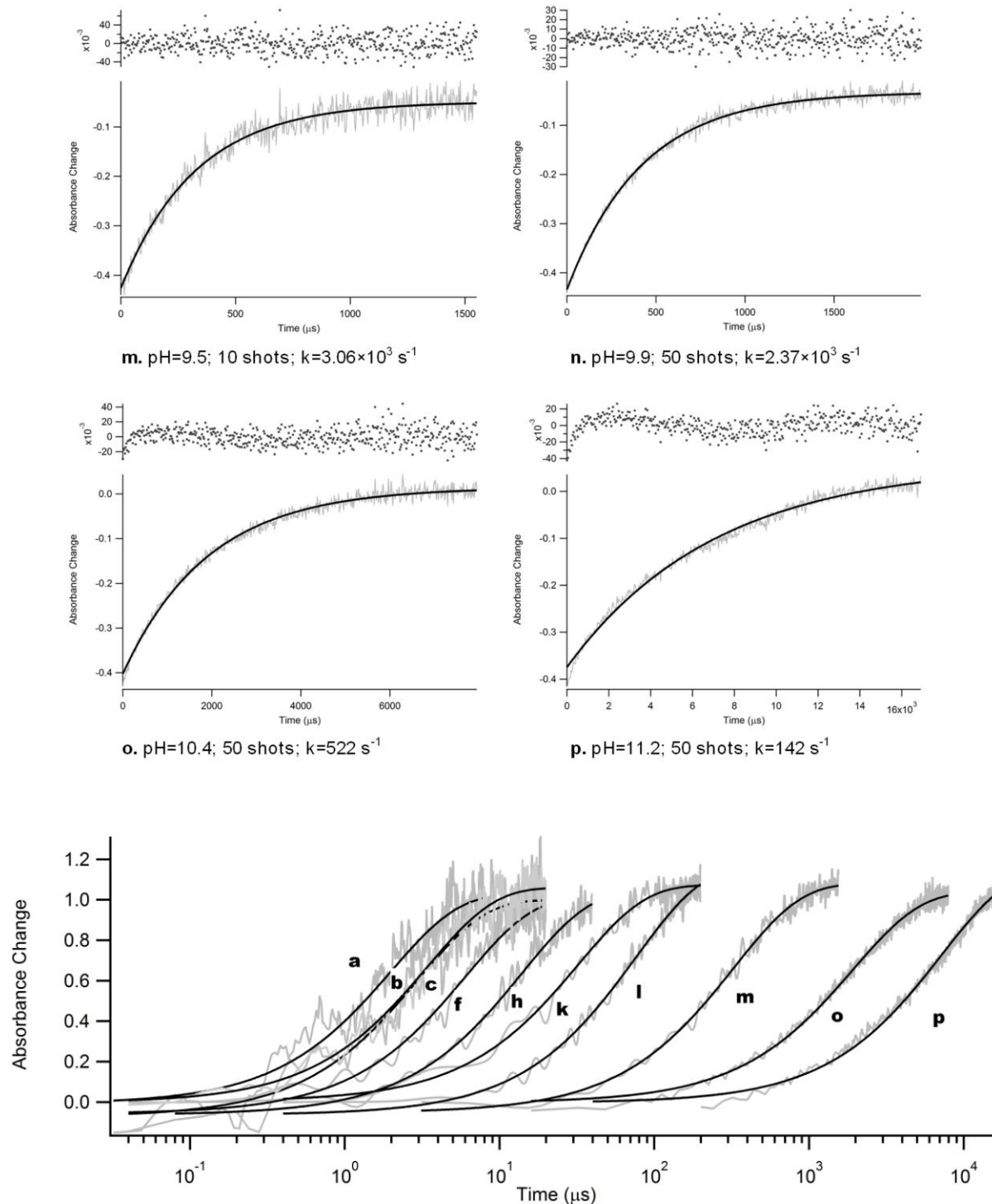


Figure S4. Thermal relaxation data for compound 4. Each panel shows data obtained at the pH indicated below the panel. Monoexponential fits are shown together with calculated residuals. The time constant obtained (k) is listed below each panel. Selected traces are shown plotted together in the final panel with a logarithmic time axis.

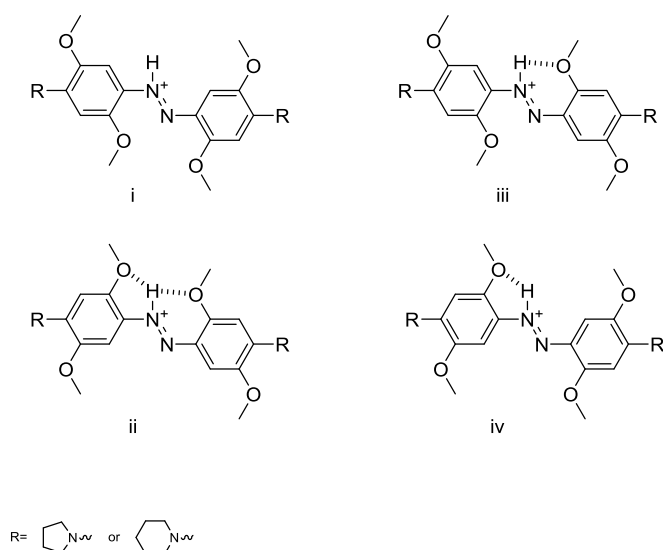
The rate constant as a function of pH is plotted in Figure 2 (main text). These data are fit to Equation 3.

$$k_{obs} = k_n * \left(\frac{10^{-pK_{cis}}}{(10^{-pH}) + (10^{-pK_{cis}})} \right) + k_{az} * \left(\frac{10^{-pH}}{(10^{-pH}) + (10^{-pK_{cis}})} \right) \quad \text{Eq. 3}$$

Where k_{obs} is the measured (fitted) rate constant at a particular pH, k_n is the rate constant for thermal isomerization of the neutral cis species, k_{az} is the rate constant for thermal isomerization of the cis azonium species and pK_{cis} refers to the cis azonium ion. Where the fit is poorly constrained due to lack of data the fit is shown as a dotted line.

Computational Methods

DFT and time-dependent DFT calculations were carried out using Gaussian 09 package.¹ Gauss View 5 was used to sketch the initial geometries by manually modifying the optimized structures of **1** in the neutral and protonated forms from our previous study.² (A table of coordinates for **1** in the neutral and protonated forms is given below). For simplicity, the piperidino analogues of **1** and **3**, and pyrrolidino analogues of **2** and **4** were used. All structures were optimized *in vacuo* using B3LYP³ hybrid functionals and the 6-31++G(d,p) basis set. Frequency calculations were performed at the same level of theory to confirm that the optimization results represented local minima on the energy landscape. An exhaustive conformational search was not carried out. For sketching the neutral structures of **3** and **4**, the *ortho* methoxy groups were placed on the opposite sides of the phenyl rings. For the protonated forms of **3** and **4**, all possible rotamers shown in Scheme 4 were calculated to determine the thermodynamically most stable geometry based on the sum of electronic and thermal free energies.



Scheme S4. Conformers with different intramolecular H-bonding patterns.

The conformers indicated by ii in Scheme 4 allowed for two hydrogen bonds and had the lowest calculated free energy after optimization. These conformers were therefore chosen for the prediction of maximum absorption wavelengths for **3** and **4**. The optimized geometries of all structures were then subjected to TD-SCF calculations using the same functionals and basis set, assuming the first 15 singlet excitations and by applying the SMD solvation model. Figure 1 shows models of each of the optimized structures in their neutral and protonated forms.

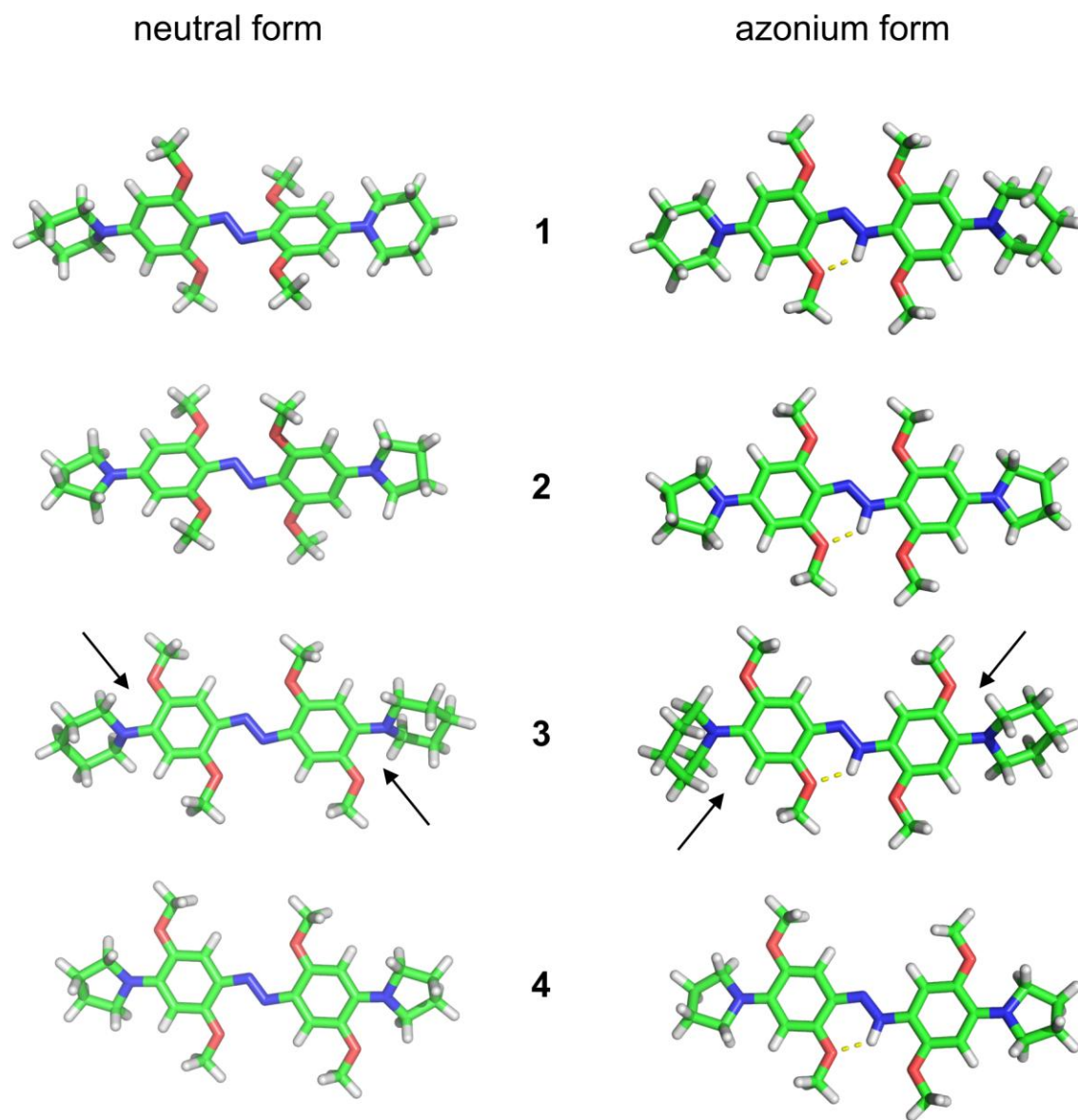


Figure S1. Models showing optimized structures of compounds **1-4** in their neutral (left column) and azonium (right column) forms. Strong H-bonds are indicated by yellow dotted lines. The steric clash leading to twisting of the 6-membered ring in **3** is highlighted by arrows. The neutral forms of **1** and **2** are highly twisted. All other compounds are relatively planar throughout the aromatic system.

Table IXYZ coordinates for **1** (neutral form)

```
70
tetraortho_6mem 0.000000
C -2.3810 -0.8700 -0.4790
C -4.0050 1.0920 0.6950
C -1.7580 0.2170 0.1960
C -3.7730 -0.9670 -0.5550
C -4.6030 0.0040 0.0360
C -2.6110 1.1950 0.7640
H -4.2230 -1.8280 -1.0280
H -4.6180 1.8650 1.1330
N 0.3870 -0.5110 0.2810
C 1.7630 -0.2320 0.2140
C 4.6040 -0.0140 0.0440
C 2.3770 0.7790 -0.5680
C 2.6230 -1.1390 0.8890
C 4.0100 -1.0260 0.8220
C 3.7740 0.8740 -0.6600
H 4.6370 -1.6770 1.4150
H 4.2110 1.6230 -1.3020
O -1.5580 -1.7760 -1.0700
O -1.9830 2.2270 1.3930
O 1.9930 -2.0830 1.6420
O 1.5510 1.5910 -1.2800
C -2.7590 3.2740 1.9520
H -3.3680 3.7790 1.1910
H -2.0400 3.9820 2.3670
H -3.4110 2.9090 2.7570
C 2.1060 2.5390 -2.1780
H 2.7170 3.2830 -1.6520
H 1.2510 3.0380 -2.6370
H 2.7080 2.0560 -2.9590
C 2.7720 -3.0620 2.3110
H 2.0540 -3.7300 2.7910
H 3.4140 -2.6120 3.0790
H 3.3900 -3.6360 1.6080
C -2.1180 -2.8040 -1.8710
H -2.7360 -3.4870 -1.2760
H -1.2660 -3.3530 -2.2760
H -2.7160 -2.3950 -2.6960
N -6.0040 -0.1590 -0.0160
C -6.8340 0.7190 0.8090
H -6.9110 1.7320 0.3640
H -6.3600 0.8250 1.7870
C -6.6020 -0.4220 -1.3350
H -5.9450 -1.0820 -1.9010
H -6.6740 0.5240 -1.9060
N 6.0110 0.1030 0.0220
C 6.5980 1.3050 -0.5700
H 6.0060 2.1680 -0.2550
H 6.5640 1.2640 -1.6770
```

C	6.7810	-1.1120	-0.2890
H	6.2990	-1.9700	0.1800
H	6.7640	-1.2940	-1.3820
C	8.2320	-0.9960	0.1840
H	8.7760	-1.9030	-0.1050
H	8.2470	-0.9390	1.2800
C	8.0500	1.4920	-0.1130
H	8.0550	1.6940	0.9660
H	8.4670	2.3760	-0.6110
C	8.9010	0.2510	-0.4080
H	9.9150	0.3750	-0.0100
H	9.0010	0.1270	-1.4960
C	-7.9940	-1.0450	-1.2090
H	-8.4150	-1.1860	-2.2130
H	-7.9010	-2.0380	-0.7500
C	-8.2420	0.1370	0.9920
H	-8.1650	-0.7870	1.5790
H	-8.8430	0.8450	1.5760
C	-8.9120	-0.1630	-0.3540
H	-9.8840	-0.6450	-0.2020
H	-9.1050	0.7810	-0.8840
N	-0.3810	0.4920	0.2470

Table II

XYZ coordinates for **1** (azonium form)

```

71
prot_tetraortho_6mem 0.000000
C -2.4500 -0.9460 -0.1370
C -4.0430 1.3570 -0.1870
C -1.7940 0.3350 -0.1540
C -3.8230 -1.0730 -0.1420
C -4.6650 0.0800 -0.1570
C -2.6640 1.4880 -0.1870
H -4.2570 -2.0570 -0.0760
H -4.6470 2.2460 -0.2620
N 0.4150 -0.3270 -0.1150
C 1.7950 -0.1380 -0.0910
C 4.6460 -0.0340 -0.0200
C 2.4740 1.1090 -0.1040
C 2.5830 -1.3210 -0.0500
C 3.9640 -1.2810 -0.0180
C 3.8690 1.1470 -0.0730
H 4.5190 -2.2020 0.0670
H 4.3560 2.1070 -0.1310
O -1.6090 -2.0170 -0.0990
O -2.0370 2.6750 -0.2360
O 1.8550 -2.4780 -0.0290
O 1.7050 2.2140 -0.1690
C -2.8060 3.8790 -0.2600
H -3.4330 3.9300 -1.1570
H -2.0760 4.6870 -0.2800

```

H	-3.4260	3.9690	0.6390
C	2.3210	3.5020	-0.1760
H	2.9070	3.6660	0.7360
H	1.4960	4.2130	-0.2120
H	2.9560	3.6340	-1.0590
C	2.5400	-3.7320	0.0040
H	1.7600	-4.4940	-0.0010
H	3.1380	-3.8280	0.9170
H	3.1760	-3.8530	-0.8790
C	-2.1420	-3.3480	-0.0870
H	-2.7440	-3.5160	0.8110
H	-1.2740	-4.0070	-0.0750
H	-2.7360	-3.5340	-0.9870
N	-6.0260	-0.0480	-0.1240
C	-6.9290	1.1000	0.0620
H	-7.3280	1.4110	-0.9170
H	-6.3720	1.9370	0.4780
C	-6.7320	-1.2590	-0.5800
H	-6.0270	-2.0750	-0.7180
H	-7.1600	-1.0400	-1.5710
N	6.0250	0.0120	0.0650
C	6.7210	1.2940	0.2350
H	6.0880	1.9620	0.8220
H	6.8920	1.7680	-0.7480
C	6.8530	-1.0210	-0.5860
H	6.2960	-1.9530	-0.6510
H	7.0590	-0.7000	-1.6220
C	8.1760	-1.2470	0.1500
H	8.7640	-1.9850	-0.4080
H	7.9700	-1.6750	1.1400
C	8.0560	1.1170	0.9710
H	7.8480	0.8160	2.0060
H	8.5580	2.0900	1.0120
C	8.9480	0.0680	0.3000
H	9.8630	-0.0860	0.8830
H	9.2600	0.4250	-0.6910
C	-7.8560	-1.6660	0.3800
H	-8.3660	-2.5440	-0.0310
H	-7.4210	-1.9620	1.3430
C	-8.0810	0.7520	1.0180
H	-7.6690	0.6040	2.0240
H	-8.7550	1.6150	1.0700
C	-8.8380	-0.5060	0.5790
H	-9.6010	-0.7690	1.3190
H	-9.3660	-0.3090	-0.3640
N	-0.4710	0.6090	-0.1430
H	0.1190	-1.3080	-0.1010

Table III

Predicted UV-Vis transitions

Structure(trans isomer)	Calculated λ_{\max}	Oscillator Strength
1 neutral	384nm, 522nm	0.666, 0.502
2 neutral	518nm, 384nm	0.638, 0.664
3 neutral	497nm	0.704
4 neutral	485nm	1.37
1 azonium	545nm	1.54
2 azonium	544nm	1.50
3 azonium rotamer i	638nm	1.20
3 azonium rotamer ii	631nm	1.34
3 azonium rotamer iii	608nm	1.33
3 azonium rotamer iv	660nm	1.24
4 azonium rotamer i	647nm	1.24
4 azonium rotamer ii	634nm	1.39
4 azonium rotamer iii	612nm	1.38
4 azonium rotamer iv	664nm	1.30

References

1. M. J. Frisch, G. W. T., H. B. Schlegel, G. E. Scuseria, M. A. Robb, J. R. Cheeseman, G. Scalmani, V. Barone, B. Mennucci, G. A. Petersson, H. Nakatsuji, M. Caricato, X. Li, H. P. Hratchian, A. F. Izmaylov, J. Bloino, G. Zheng, J. L. Sonnenberg, M. Hada, M. Ehara, K. Toyota, R. Fukuda, J. Hasegawa, M. Ishida, T. Nakajima, Y. Honda, O. Kitao, H. Nakai, T. Vreven, J. A. Montgomery, Jr., J. E. Peralta, F. Ogliaro, M. Bearpark, J. J. Heyd, E. Brothers, K. N. Kudin, V. N. Staroverov, R. Kobayashi, J. Normand, K. Raghavachari, A. Rendell, J. C. Burant, S. S. Iyengar, J. Tomasi, M. Cossi, N. Rega, J. M. Millam, M. Klene, J. E. Knox, J. B. Cross, V. Bakken, C. Adamo, J. Jaramillo, R. Gomperts, R. E. Stratmann, O. Yazyev, A. J. Austin, R. Cammi, C. Pomelli, J. W. Ochterski, R. L. Martin, K. Morokuma, V. G. Zakrzewski, G. A. Voth, P. Salvador, J. J. Dannenberg, S. Dapprich, A. D. Daniels, Ö. Farkas, J. B. Foresman, J. V. Ortiz, J. Cioslowski, and D. J. Fox, *Gaussian 09, Revision B.01*, (2009) Gaussian, Inc., Wallingford CT.
2. S. Samanta, A. Babalhavaeji, M. X. Dong and G. A. Woolley, *Angew. Chem. Int. Ed. Engl.*, 2013, **52**, 14127-14130.
3. A. D. Becke, *J. Chem. Phys.*, 1997, **98**, 5648-5652.